THE BELL SYSTEM TECHNICAL JOURNAL
Vol. 53, No. 9, November 1974
Printed in U.S.A.

Reduction of Multimode Pulse Dispersion by Intentional Mode Coupling

By D. MARCUSE

(Manuscript received May 3, 1974)

Guidelines for the design of multimode, step-index fibers with intentional fluctuations of the refractive index of the core are given, with the aim of reducing multimode pulse dispersion. It appears possible to engineer a fiber with carefully designed refractive index fluctuations, the azimuthal variation of which is governed by the function cos ϕ and the z dependence of which has a spatial Fourier spectrum with a sharp cutoff frequency. By limiting the location of the index fluctuations to a region below a certain radius r_{max}, coupling to modes with large azimuthal mode numbers can be avoided and power loss via coupling to radiation modes can be held to a minimum.

I. INTRODUCTION

Optical fibers supporting many guided modes suffer from multimode dispersion. A pulse launched into a multimode fiber excites many modes, each traveling at a different group velocity. At the far end of the fiber the pulse is spread out in time because of the different group delays of each mode. This multimode dispersion effect is usually more serious than the single-mode dispersion caused by the dispersive effect of the dielectric material of the waveguide core and by the inherently dispersive nature of mode guidance. Discussions of multimode dispersion in the absence of mode coupling can be found in Refs. 1, 2, and 3.

S. D. Personick discovered that multimode dispersion in fibers can be reduced by intentional (or unintentional) mode coupling. If the power carried in the fiber transfers back and forth between slow and fast modes, averaging takes place, so that the pulse no longer breaks up into a sequence of pulses but is forced to travel at an average group delay with a concomitant reduction in pulse spreading. Although the spread of a pulse carried by uncoupled modes is proportional to the

length of the fiber, it only becomes proportional to the square root of its length if the pulses are coupled among each other.[3–5]

However, reduction of multimode pulse dispersion by means of mode coupling must be bought at a price. Any mechanism that causes coupling among the guided modes also tends to couple guided modes to the continuum of radiation modes. Power coupled into radiation modes radiates away causing losses. Radiation loss can be reduced by careful control of the coupling process.[5] It is possible, at least in principle, to provide strong coupling among the guided modes but only very little coupling to radiation modes. The loss penalty can thus be controlled and kept to small amounts.[3,5]

Coupling between two fiber modes is caused by a specific spatial frequency of the Fourier spectrum of the coupling function. Two modes couple via a spatial frequency that is equal to the difference of the propagation constants of the two modes. Control of the loss penalty for multimode dispersion is thus possible by shaping the Fourier spectrum of the coupling function. In general, it is desirable to achieve a spectrum that provides a sufficient number of spatial frequencies below a critical frequency and a sharp cutoff of the spectrum at the critical spatial frequency.[3,5]

In this paper we discuss means of mode coupling by employing intentional fluctuations of the refractive index of a fiber whose unperturbed core has a constant index of refraction (step-index fibers). It is necessary to shape the core-index fluctuations so that only modes with adjacent azimuthal mode numbers ν couple to each other. Additional control of the coupling process must be provided by a sharp cutoff of the coupling spectrum that can be achieved by careful design of the z dependence (z is the axial direction) of the index fluctuations. Finally, radiation losses can be minimized by limiting the index fluctuations to a region near the fiber axis.

The paper begins with a discussion of the requirements on the Fourier spectrum imposed by the desire to minimize the loss penalty. Next we provide explicit expressions for the power-coupling coefficients and estimate the amount of index fluctuation that is necessary to achieve a desired reduction in multimode dispersion.

This discussion is intended as a guide to the fiber designer, pointing out the possibilities available for reduction of multimode dispersion and explaining the difficulties that must be overcome.

II. SHAPING THE SPATIAL FOURIER SPECTRUM

We consider two modes with propagation constants β_i and β_j. Interaction between these modes is described by a coupling coefficient that

depends on the distortion of the core boundary or on refractive-index irregularities. The azimuthal symmetry of the irregularity provides selection rules for the coupling process. The z dependence of the irregularity enters the coupling process via its spatial Fourier spectrum. A sinusoidal component of the Fourier spectrum of the form

$$F(\theta) \cos \theta z \tag{1}$$

couples the two modes only if the relation[3,6]

$$|\beta_i - \beta_j| = \theta \tag{2}$$

is satisfied. (This requirement stems from first-order perturbation theory and is valid provided that the coupling is weak.)

It is not hard to envision a sufficient number of spatial frequencies that couple all modes among each other. However, as pointed out in Section I, coupling to radiation modes causes power loss by radiation from the fiber core.[3,6] It is thus essential to avoid coupling between guided and radiation modes. To see whether this is possible, we must study the spacing (in β space) between the guided modes. I have computed the propagation constants of all the guided modes for a step-index fiber with

$$V = (n_1^2 - n_2^2)^{\frac{1}{2}} ka = 40, \tag{3}$$

where n_1 = refractive index of fiber core, n_2 = index of cladding, k = free-space propagation constant, a = fiber core radius. The propagation constants were obtained as solutions of the simplified eigenvalue equation of the optical fiber.[1,3] When the propagation constants are listed in order of their numerical values, regardless of mode number, they appear approximately evenly spaced. This behavior of the propagation constants of fiber modes contrasts with the behavior of the modes of a dielectric slab. Here we find that the spacings between modes increase monotonically so that the spatial frequencies, required to couple nearest neighbors, also increase.[3] By providing a cutoff to the Fourier spectrum of spatial frequencies contained in the coupling function, we can provide coupling among lower-order modes of the slab and uncouple either the last guided mode or a few of the higher-order guided modes, depending on the value of the spatial cutoff frequency (see Fig. 1). Once the highest-order (or a few high-order) guided modes are uncoupled from the rest, there is no danger of incurring radiation loss caused by the coupling process. Things are not quite that simple in the round optical fiber because the modes are not naturally arranged with ever-increasing spacings between neighbors.

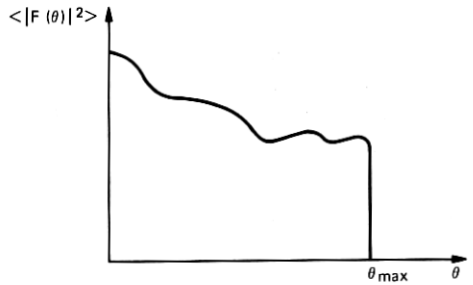

Fig. 1—Schematic drawing of the desired spatial Fourier spectrum of the z dependence of the index fluctuations. The shape of the function is unimportant except for its abrupt cutoff.

A good approximation to the actual solution of the eigenvalue equation is obtained if we approximate the Bessel function by the formula[7]

$$J_\nu(x) = \sqrt{\frac{2}{\pi}} \frac{\cos\left[(x^2 - \nu^2)^{\frac{1}{2}} - \nu \arccos\left(\frac{\nu}{x}\right) - \frac{\pi}{4}\right]}{(x^2 - \nu^2)^{\frac{1}{4}}}. \tag{4}$$

In weakly guiding fibers the transverse electric field component can be represented as [1,3]

$$E_y = AJ_\nu(\kappa r) \cos(\nu\phi) e^{-i\beta z}, \tag{5}$$

with

$$\kappa = (n_1^2 k^2 - \beta^2)^{\frac{1}{2}}. \tag{6}$$

To a good approximation, we may assume that $E_y = 0$ at the core radius $r = a$. This approximation is better for modes far from their cutoff value but it gives a reasonable indication of the propagation constants for practically all modes. An approximate eigenvalue equation of the guided modes thus follows from (4),

$$[(\kappa a)^2 - \nu^2]^{\frac{1}{2}} - \nu \arccos\left(\frac{\nu}{\kappa a}\right) - \frac{\pi}{4} = (2m - 1)\frac{\pi}{2} \tag{7}$$

for $m = 1, 2, 3, \cdots$. By regrouping this equation we obtain a form that is useful for iterative solutions,

$$\kappa a = \left\{\nu^2 + \left[(m - \tfrac{1}{4})\pi + \nu \arccos\left(\frac{\nu}{\kappa a}\right)\right]^2\right\}^{\frac{1}{2}}. \tag{8}$$

Using (6) and (7) we derive the following approximate expression for

the spacing between guided modes,

$$\Delta\beta = -\frac{\kappa^2}{\beta}\left\{\frac{\Delta\nu}{\nu} + \frac{\pi\Delta m - \frac{\Delta\nu}{\nu}(m - \frac{1}{4})\pi}{[(\kappa a)^2 - \nu^2]^{\frac{1}{2}}}\right\}. \tag{9}$$

$\Delta\beta$ is the spacing between modes that are separated by an amount $\Delta\nu$ of the azimuthal mode number ν and by a change Δm of the radial mode number m.

If we place no restriction on the allowed values of $\Delta\nu$ or Δm, it is impossible to shape the spatial Fourier spectrum of the coupling function so that coupling to radiation modes is avoided. It is thus necessary to introduce definite "selection rules" for the coupling among the guided modes. We shall see later that it is possible to shape the refractive-index distribution or the deformation of the core-cladding boundary such that only modes with

$$\Delta\nu = \pm 1 \tag{10}$$

can couple to each other. We shall thus assume that the selection rule (10) is enforced and continue our discussion on this assumption. The allowed values for Δm remain arbitrary. However, it is true that the spatial frequencies for coupling between modes (that is, the value of $\Delta\beta$) are larger for larger values of Δm. Since it is our aim to introduce a cutoff frequency into the spatial Fourier spectrum so that modes with large spatial frequency separation will be uncoupled, we restrict the discussion also to a limited range of values for Δm and consider only the case

$$\Delta m = 0 \quad \text{or} \quad \pm 1. \tag{11}$$

Using (10) and taking $\Delta m = 0$ we obtain from (9)

$$|\Delta\beta| = \frac{\kappa^2}{\nu\beta}\left|\frac{(m - \frac{1}{4})\pi}{[(\kappa a^2) - \nu^2]^{\frac{1}{2}}} - 1\right| \quad \text{for} \quad \begin{matrix}\Delta m = 0 \\ \Delta\nu = \pm 1.\end{matrix} \tag{12}$$

For $\Delta m = \pm 1$ we obtain from (10) and (9)

$$|\Delta\beta| = \frac{\kappa^2}{\nu\beta}\left|\frac{[(m - \frac{1}{4}) + \nu]\pi}{[(\kappa a)^2 - \nu^2]^{\frac{1}{2}}} - 1\right| \quad \text{for} \quad \begin{matrix}\Delta m = -\Delta\nu \\ \Delta\nu = \pm 1\ .\end{matrix} \tag{13}$$

The case $\Delta m = +\Delta\nu$ has been excluded since it leads to larger spatial frequencies than those obtained from (13).

Figures 2 and 3 illustrate the boundaries of various regions in mode-number space ν, m. Both figures were drawn for $V = 40$ [see eq. (3)], $n_1 = 1.515$, and $n_2 = 1.5$ so that $n_1/n_2 = 1.01$. The solid line delineates

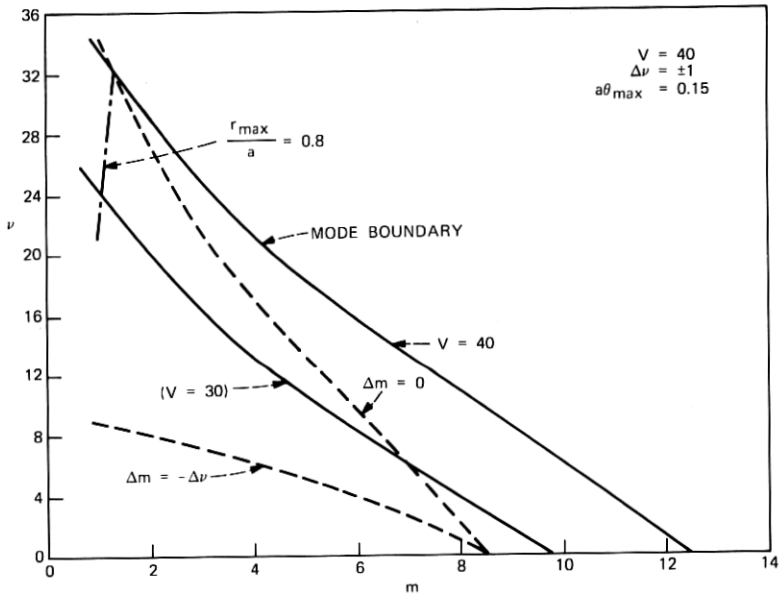

Fig. 2—Various regions in mode-number space ν, m. All curves belong to $V = 40$, $n_2 = 1.5$, and $n_1/n_2 = 1.01$ with the exception of the solid line labeled $(V = 30)$. The solid lines indicate the boundaries of the range of guided modes for the respective V values. The broken line labeled $\Delta m = 0$ delineates the area below which coupling of modes with the selection rule $\Delta\nu = \pm 1$ and $\Delta m = 0$ is possible. The broken line labeled $\Delta m = -\Delta\nu$ limits the range of coupling with the selection rule $\Delta\nu = \pm 1$, $\Delta m = -\Delta\nu$. The dash-dotted line is the limit of the coupling range caused by the location of $r = r_{max} = 0.8a$. The spatial Fourier spectrum cuts off at $\theta_{max}a = 0.15$.

the boundary of guided modes; it is obtained by plotting those values of ν and m that result in $\kappa a = V$ [see eq. (14)]. All guided modes are located to the left and below the solid line. The broken lines* represent lines of constant spatial frequency. They result from plotting the combinations of ν and m values that result in $\Delta\beta = \theta_{max}$. The line labeled $\Delta m = 0$ was computed from (12) and the line $\Delta m = -\Delta\nu$ was obtained from (13). The broken lines delineate the boundaries for mode coupling with the spatial Fourier spectrum of the coupling function of Fig. 1, the cutoff frequency of which is $\theta = \theta_{max}$. Modes below and to the left of the broken lines couple to their nearest neighbors via the selection rule $\Delta\nu = \pm 1$ and $\Delta m = 0$ or $\Delta m = -\Delta\nu$. Modes located to the right and above the broken lines cannot couple to each other

* The meaning of the dash-dotted lines and the solid line labeled $(V = 30)$ will be explained later.

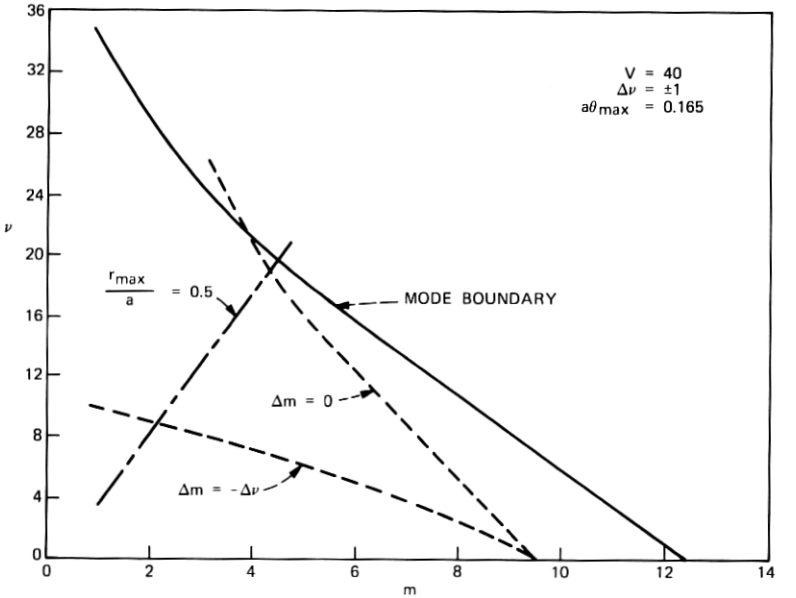

Fig. 3—Same as Fig. 2 except that $\theta_{max}a = 0.165$, $r_{max} = 0.5a$.

since no spatial frequencies achieving this coupling are available. Figures 2 and 3 differ only in the choice of the cutoff frequency θ_{max}. There are no transitions with $\Delta\nu = \pm 1$ that couple via smaller spatial frequencies than the ones indicated in the figures. It is thus apparent that it is possible to provide coupling among most guided modes by means of the Fourier spectrum shown in Fig. 1. However, modes to the right and above the uppermost broken line remain uncoupled. It is necessary to uncouple a few higher-order modes in order to avoid coupling into the continuum of radiation modes. The conditions shown in Fig. 2 achieve this goal almost completely. Only the mode $m = 1$, $\nu = 34$, lying on the boundary of the guided-mode region, is coupled to radiation modes as well as the other guided modes. Power is thus able to flow out of the guided-mode region causing radiation losses via this one guided mode. This power loss could be avoided by decreasing θ_{max}.

The conditions prevailing in Fig. 3 would result in a high loss penalty since all modes with $m < 4$, $\nu > 21$ on the boundary of the guided-mode region couple to guided as well as radiation modes. However, we shall show later that it is possible to prevent mode coupling for modes exceeding a certain maximum ν value that can be chosen by a suitable

design of the intentional index fluctuations. It is thus possible to achieve a low loss penalty even for the conditions shown in Fig. 3 provided the coupling mechanism is carefully designed to avoid coupling for modes with $\nu > 20$.

Modes located between the two broken lines in Figs. 2 and 3 can couple only to their neighbors above and below in the mode-number plane. However, since the members with low ν values below the line $\Delta m = -\Delta\nu$ are able to couple to their neighbors to the left and to the right, all modes below the uppermost broken line are actually coupled together.

We can give an approximate rule for calculating the spatial cutoff frequency appearing in Figs. 2 and 3. We begin by specifying the maximum ν value on the mode boundary for which mode coupling should cease. As mentioned earlier, the design specification for this value $\nu_{\max}$ will be given in the section on mode coupling. Next we need to know the corresponding value of m on or near the mode boundary—the solid line in Figs. 2 and 3. We obtain it from the cutoff condition $\kappa a = V$ and (8),

$$m_{\max} = \frac{1}{4} - \frac{\nu_{\max}}{\pi} \arccos\left(\frac{\nu_{\max}}{V}\right) + \frac{1}{\pi}(V^2 - \nu_{\max}^2)^{\frac{1}{2}}. \tag{14}$$

Substitution of $\nu_{\max}$ and $m_{\max}$ into (12) using $\beta = n_2 k$ yields the desired value for $\Delta\beta = \theta_{\max}$. For $V = 40$ and $\nu_{\max} = 20$ we obtain from (14) $m_{\max} = 4.61$ and from (12) $\theta_{\max} a = 0.17$ in agreement with Fig. 3. Of course, it does not make physical sense to use a noninteger $m_{\max}$, but it is advisable to use this value in (12) in order to obtain a more accurate value of $\theta_{\max}$. Incidentally, (14) defines the mode boundary if we use it for all possible values $\nu = \nu_{\max}$.

III. POWER COUPLING COEFFICIENTS

Mode coupling in multimode dielectric optical waveguides is most conveniently described by a coupled-mode theory. The power coupling coefficients are defined as follows:[3,5]

$$h_{\nu n,\mu m} = \langle |K_{\nu n,\mu m}|^2 \rangle. \tag{15}$$

The symbol $\langle\ \rangle$ indicates an ensemble average. The coefficient $K_{\nu n,\mu m}$ stems from the coupled amplitude equations and is defined as[8]

$$K_{\nu n,\mu m} = \frac{\omega \epsilon_0}{4iP} \int_0^{2\pi} d\phi \int_0^{\infty} r dr (n^2 - n_0^2) \mathcal{E}_{\nu n}^* \cdot \mathcal{E}_{\mu m}. \tag{16}$$

The angular frequency of the radiation is ω, ϵ_0 is the dielectric permit-

tivity of vacuum, and P designates the power normalization constant of the modes, the electric field vectors of which are indicated by script letters. The refractive-index distribution of the actual guide with index fluctuations is n while n_0 indicates the index distribution of a perfect guide from which the actual guide deviates only slightly. Our interest is focused on introducing intentional index fluctuations for the purpose of mode coupling. We are thus free to choose n to achieve our goal. It was pointed out earlier that coupling to radiation modes is unavoidable unless certain selection rules are imposed on the coupling process. Our discussion in the last section was based on the selection rule $\Delta\nu = \pm 1$. To achieve this selection rule we must require that the refractive-index distribution be of the following general form:

$$n^2 - n_0^2 = 2n_1\Delta n g(r) f(z) \cos\phi. \tag{17}$$

We know from earlier work that the ϕ-dependence of this index distribution leads to the desired selection rule.[9]

We found in the preceding section that it is also desirable to avoid coupling among modes with large ν values. It follows from the properties of Bessel functions that the field intensity of the transverse field components is very weak for radii that obey the relation

$$\kappa r < \nu.$$

This result is easily interpreted in terms of ray optics. Modes with large values of ν are represented by skew rays that spiral around the fiber axis. These rays avoid the vicinity of the waveguide axis and stay nearer to the core boundary for larger values of ν. The radius defined by $\kappa r = \nu$ represents the turning point below which a ray with a given value of ν does not penetrate. The coupling formula (16) shows that mode coupling depends on the field strength at the point where the index irregularity is located. By providing refractive-index variations that do not extend beyond a radius r_{max}, it is possible to limit mode coupling to modes whose ν values remain below a maximum value near the mode boundary that is defined as

$$\nu_{max} = V\frac{r_{max}}{a}. \tag{18}$$

κa has been replaced by its maximum value V. The values of ν_{max} and the corresponding values for m_{max} and θ_{max} defined by (14) and (12) determine the position at which the dotted curves labeled $\Delta m = 0$ cross the solid curves in Figs. 2 and 3 that define the guided-mode boundary in mode-number space. Coupling of guided modes to radia-

tion modes can be avoided by limiting the ν values of those modes that are coupled by index fluctuations. If the intentional index fluctuations do not extend beyond the radius $r_{\max}$, coupling is restricted to those modes that remain below a boundary defined by the equation

$$\nu = \kappa r_{\max}. \tag{19}$$

If we combine this equation with formula (8) we obtain the function $m = m(\nu)$ that defines the boundary in mode-number space beyond which mode coupling ceases, because the index fluctuations are restricted to radii $r \leqq r_{\max}$,

$$m = \frac{1}{4} + \frac{\nu}{\pi}\left\{\left(\frac{a^2}{r_{\max}^2} - 1\right)^{\frac{1}{2}} - \arccos\frac{r_{\max}}{a}\right\}. \tag{20}$$

This boundary is shown as a dash-dotted line in Figs. 2 and 3. We now have the means of providing coupling among all guided modes that remain inside the nearly triangular areas that are bounded by the dotted lines labeled $\Delta m = 0$ and the dash-dotted lines in Figs. 2 and 3. If these areas remain below the guided-mode boundary (the solid line labeled $V = 40$ in Fig. 2), coupling to radiation modes can be avoided.

After this digression into the fundamental properties of mode coupling we proceed with the derivation of specific coupling formulas. Substitution of the field vectors, given by (5) and in more detail by Ref. 3, into (16) we obtain with the help of (17)

$$K_{\nu n,\mu m} = \frac{k\gamma_{\nu n}\gamma_{\mu m} f(z)\int_0^a rg(r)J_\nu(\kappa_{\nu n}r)J_\mu(\kappa_{\mu m}r)dr}{2in_1V^2\left|J_{\nu-1}(\kappa_{\nu n}a)J_{\nu+1}(\kappa_{\nu n}a)J_{\mu-1}(\kappa_{\mu m}a)J_{\mu+1}(\kappa_{\mu m}a)\right|^{\frac{1}{2}}}\delta_{\nu\pm1,\mu}. \tag{21}$$

The parameter $\gamma_{\nu n}$ is defined as

$$\gamma_{\nu n} = (\beta_{\nu n}^2 - n_2^2k^2)^{\frac{1}{2}} \tag{22}$$

and $\delta_{\nu\mu}$ is Kronecker's delta symbol.

Of the many possible choices for the function $g(r)$ we use only two examples that may be of particular practical interest. First we use

$$g(r) = W\delta(r - r_{\max}). \tag{23}$$

W is the very narrow width of the ring of index fluctuations. We substitute this equation into (21) but proceed immediately to the power coupling coefficient (15). The Fourier spectrum is defined as

$$F(\theta) = \lim_{L\to\infty}\frac{1}{\sqrt{L}}\int_0^L f(z)e^{-i\theta z}dz \tag{24}$$

and the power coupling coefficient for a narrow, ring-shaped refractive-index fluctuation is given as

$$h_{\nu n,\mu m} = \left\{ \frac{\Delta n W k r_{\max} \gamma_{\nu n} \gamma_{\mu m} J_\nu(\kappa_{\nu n} r_{\max}) J_\mu(\kappa_{\mu m} r_{\max})}{V^2 J_{\nu-1}(\kappa_{\nu n} a) J_{\mu-1}(\kappa_{\mu m} a)} \right\}^2 \langle |F|^2 \rangle \delta_{\nu \pm 1,\mu}. \quad (25)$$

Because the relation

$$J_\nu(\kappa_{\nu n} a) \approx 0 \quad (26)$$

is approximately valid we have used

$$J_{\nu+1}(\kappa_{\nu n} a) = -J_{\nu-1}(\kappa_{\nu n} a). \quad (27)$$

As a second example we consider the function

$$g(r) = \begin{cases} 1 & \text{for } r < r_{\max} \\ 0 & \text{for } r > r_{\max}. \end{cases} \quad (28)$$

Limiting the index fluctuations to a wide range, $0 < r < r_{\max}$. In this case the power coupling coefficient assumes the form

$$h_{\nu n,\mu m} = \left\{ \frac{\Delta n k r_{\max} \gamma_{\nu n} \gamma_{\mu m} [\kappa_{\mu m} J_\nu(\kappa_{\nu n} r_{\max}) J_{\mu-1}(\kappa_{\mu m} r_{\max}) - \kappa_{\nu n} J_{\nu-1}(\kappa_{\nu n} r_{\max}) J_\mu(\kappa_{\mu m} r_{\max})]}{V^2 [\kappa_{\nu n}^2 - \kappa_{\mu m}^2] J_{\nu-1}(\kappa_{\mu n} a) J_{\nu-1}(\kappa_{\mu m} a)} \right\}^2 \cdot \langle |F|^2 \rangle \delta_{\nu \pm 1,\mu}. \quad (29)$$

The argument of the power spectrum $\langle |F^2| \rangle$ in (25) and (29) is $\beta_{\nu n} - \beta_{\mu m}$.

IV. PULSE WIDTH REDUCTION BY INTENTIONAL MODE COUPLING

Random coupling of the modes of a multimode fiber causes the many pulses, traveling on different guided modes at different group velocities, to be coupled together so that an equilibrium pulse establishes itself traveling at an average group velocity. Its ensemble average has a gaussian shape[3,5] the width of which is given by the formula[10]

$$T = 4(\rho_2 L)^{\frac{1}{2}}, \quad (30)$$

with[11]

$$\rho_2 = \sum_{i=2}^{N} \frac{\left[\sum_{\nu=1}^{N} B_\nu^{(1)} \left(\frac{1}{v_\nu} - \frac{1}{v_a} \right) B_\nu^{(i)} \right]^2}{\rho_0^{(i)} - \rho_0^{(1)}}. \quad (31)$$

Equation (30) shows that the width of the pulse grows proportionally to the square root of the length L of the fiber. The parameter ρ_2 is the second perturbation of the first eigenvalue that results from an algebraic eigenvalue problem, $B_\nu^{(i)}$ are the components of the ith eigen-

vector, $\rho_0^{(i)}$ is the ith eigenvalue of zero order, and v_ν and v_a are the group velocity of mode ν and the average group velocity.

The evaluation of this expression is difficult. If only a few guided modes exist, computer solutions of the eigenvalues and eigenvectors can be obtained. If many modes are guided, it is possible to convert the algebraic eigenvalue problem to a partial differential equation, provided that it can be assumed that only nearest neighbors couple among each other.[3,12] For modes close to the edge of the coupling range, indicated by the dotted lines in Figs. 2 and 3, the assumption of nearest-neighbor coupling is well justified since the spatial Fourier spectrum of the coupling function lacks the higher frequencies required to couple a mode to a neighbor farther away. However, the lower-order modes are crowded more closely so that there are spatial frequencies available for coupling to modes other than the nearest neighbors. This increase in coupling strength is partially compensated for by the fact that modes above the dotted line labeled $\Delta m = -\Delta\nu$ in Figs. 2 and 3 can couple only vertically. In order to be able to give an order-of-magnitude estimate of the index fluctuations required to achieve a certain reduction of the pulse width, we shall assume that nearest-neighbor coupling can be assumed and provide an expression for the pulse width reduction that may be regarded as a crude approximation.

We use the theory presented in Ref. 3. The only modification necessary to the formulas presented in Section 5.6 of Ref. 3 consists in the realization that our coupling scheme avoids radiation losses, so that the highest-order members of the group of coupled modes are not depleted contrary to the assumption in Ref. 3. The eigenvectors and eigenvalues defined on p. 235 of Ref. 3 can be used, except that the first eigenvector is now constant, independent of the mode number. All eigenvectors are mutually orthogonal and properly normalized. Using the procedure explained in Ref. 3 we obtain the result

$$R = \frac{T}{\Delta\tau} = \frac{0.225V}{(Lh)^{\frac{1}{2}}}. \tag{32}$$

T is the full width at the $1/e$ points of the gaussian-shaped pulse, $\Delta\tau$ is the width of the pulse train that would exist in the absence of coupling, V is the normalized frequency parameter defined by (3), L is the length of the fiber, and h the power coupling coefficient. It was assumed that only nearest neighbors couple to each other and the strength of these coupling coefficients was assumed to be identical for all the modes.

R is the improvement factor that indicates the reduction of the length of the pulse relative to its uncoupled length. It is thus desirable to achieve as small a value of R as possible. Values of $R > 1$ do not describe a physically meaningful situation. The formula may result in values $R > 1$. This indicates that the coupling is not strong enough to achieve an equilibrium pulse in the length of fiber available.

We are discussing numerical values for the two types of couplings described by (25) and (29). Values have been computed for

$$\bar{h}_{\nu n;\nu+1,m} = \left[\frac{\gamma_{\nu n} a \gamma_{\nu+1,m} a J_\nu(\kappa_{\nu n} r_{\max}) J_{\nu+1}(\kappa_{\nu+1,m} r_{\max})}{J_{\nu-1}(\kappa_{\nu n} a) J_\nu(\kappa_{\nu+1,m} a)} \right]^2 \tag{33}$$

and

$$\bar{H}_{\nu n;\nu+1,m} = \left\{ \frac{\gamma_{\nu n} a \gamma_{\nu+1,m} a [\kappa_{\nu+1,m} J_\nu(\kappa_{\nu n} r_{\max}) J_\nu(\kappa_{\nu+1,m} r_{\max}) - \kappa_{\nu n} J_{\nu-1}(\kappa_{\nu n} r_{\max}) J_{\nu+1}(\kappa_{\nu+1,m} r_{\max})]}{a(\kappa_{\nu n}^2 - \kappa_{\nu+1,m}^2) J_{\nu-1}(\kappa_{\nu n} a) J_\nu(\kappa_{\nu+1,m} a)} \right\}^2 \tag{34}$$

for all the modes of a fiber with $V = 40$, $n_1 = 1.515$, and $n_1/n_2 = 1.01$. A few sample values are listed in Tables I and II. The values listed

Table I — Sample values of normalized coupling coefficients for a narrow ring of refractive-index fluctuations located at $r = r_{\max}$ with $r_{\max}/a = 0.8$

ν	n	$\bar{h}_{\nu n;\nu+1,n}$	$\bar{h}_{\nu n;\nu+1,n-1}$
1	1	$2.212\ 10^6$	0.
1	2	$4.608\ 10^6$	$3.987\ 10^5$
1	3	$1.023\ 10^6$	$2.879\ 10^6$
1	4	$1.287\ 10^3$	$7.733\ 10^4$
1	5	$4.780\ 10^5$	$5.678\ 10^3$
1	6	$3.844\ 10^6$	$1.931\ 10^6$
1	7	$2.726\ 10^6$	$4.107\ 10^6$
1	8	$7.018\ 10^4$	$8.497\ 10^5$
1	9	$2.262\ 10^4$	$5.610\ 10^3$
1	10	$2.431\ 10^6$	$5.888\ 10^5$
1	11	$4.236\ 10^6$	$4.181\ 10^6$
1	12	$3.964\ 10^5$	$2.115\ 10^6$
10	1	$4.945\ 10^7$	0.
10	2	$7.071\ 10^3$	$1.981\ 10^5$
10	3	$1.597\ 10^7$	$8.981\ 10^5$
10	4	$1.517\ 10^7$	$1.841\ 10^7$
10	5	$1.321\ 10^5$	$2.600\ 10^6$
10	6	$1.467\ 10^6$	$1.451\ 10^5$
10	7	$3.179\ 10^7$	$9.235\ 10^6$
10	8	$4.896\ 10^7$	$4.112\ 10^7$
20	1	$5.807\ 10^7$	0.
20	2	$3.229\ 10^8$	$1.227\ 10^8$
20	3	$4.017\ 10^7$	$1.360\ 10^8$
20	4	$4.954\ 10^7$	$2.556\ 10^7$

Table II — Sample values of normalized coupling coefficients for a wide band of refractive-index fluctuations extending from $r = 0$ to $r = r_{max}$ with $r_{max}/a = 0.8$

ν	n	$\bar{H}_{\nu n;\nu+1,n}$	$\bar{H}_{\nu n;\nu+1,n-1}$
1	1	$6.078\ 10^4$	0.
1	2	$1.141\ 10^5$	$1.349\ 10^4$
1	3	$8.734\ 10^4$	$6.439\ 10^4$
1	4	$4.845\ 10^4$	$8.157\ 10^4$
1	5	$4.439\ 10^4$	$5.351\ 10^4$
1	6	$6.481\ 10^4$	$3.728\ 10^4$
1	7	$7.628\ 10^4$	$4.844\ 10^4$
1	8	$6.336\ 10^4$	$6.806\ 10^4$
1	9	$5.318\ 10^4$	$6.709\ 10^4$
1	10	$6.474\ 10^4$	$5.431\ 10^4$
1	11	$8.767\ 10^4$	$5.794\ 10^4$
1	12	$1.136\ 10^5$	$8.628\ 10^4$
10	1	$1.817\ 10^5$	0.
10	2	$5.642\ 10^4$	$8.361\ 10^5$
10	3	$1.215\ 10^5$	$2.730\ 10^5$
10	4	$1.652\ 10^5$	$3.173\ 10^5$
10	5	$1.377\ 10^5$	$4.373\ 10^5$
10	6	$1.627\ 10^5$	$4.063\ 10^5$
10	7	$3.429\ 10^5$	$4.248\ 10^5$
10	8	$1.299\ 10^6$	$9.413\ 10^5$
20	1	$7.904\ 10^4$	0.
20	2	$5.450\ 10^5$	$1.264\ 10^6$
20	3	$6.717\ 10^5$	$4.260\ 10^6$
20	4	$2.118\ 10^6$	$7.286\ 10^6$

in Table I fluctuate because the narrow band of refractive-index variations may occasionally find itself located near a node of one of the two field functions so that the coupling coefficient can even vanish for a certain pair of modes. For this reason it is advisable to provide at least two bands of the kind (23) at different radii. The coupling coefficients for the second case, listed in Table II, corresponding to a wide band of refractive-index fluctuations, show far less variations. For want of a better procedure we use average values of the coupling coefficients in (32). It may be expected that the low values of the coupling coefficients determine the rate at which power is exchanged among the modes. On the other hand, we know that more than just nearest neighbors couple for low values of ν and n. In order to achieve an order-of-magnitude estimate we use the arithmetic mean of the entries in the first block of data in the tables for $\nu = 1$ and obtain for the average value of the coupling coefficient h from Table I and (25)

$$h = 2 \times 10^6 \left(\frac{\Delta n k r_{max}}{a V^2} \right)^2 \frac{W^2}{a^2} \langle |F|^2 \rangle. \tag{35}$$

Likewise, we find from Table II and (29)

$$h = 7 \times 10^4 \left(\frac{\Delta n k r_{\max}}{a V^2} \right)^2 \langle |F|^2 \rangle. \tag{36}$$

It is clear that (35) and (36) hold only for the special case $V = 40$, $n_1 = 1.515$, and $n_1/n_2 = 1.01$. These values correspond to a fiber with radius $a = 30\ \mu$m if the free-space wavelength is assumed to be $\lambda_0 = 1\ \mu$m.

We are now asking for a pulse width reduction of $R = 0.1$ in a fiber whose length is $L = 1$ km. From (32) and (36) we obtain with $r_{\max} = 0.8a$

$$(\Delta n)^2 \langle |F|^2 \rangle = 4 \times 10^{-7} a. \tag{37}$$

The value obtained from (32) and (35) is identical with (37) if

$$W/a = 0.19. \tag{38}$$

It is apparent from (37) that it is the product of $(\Delta n)^2$ with the amplitude of the spatial power spectrum [of the z dependence of the index fluctuations $f(z)$] that determines the effectiveness of the index fluctuations for reducing pulse dispersion. We relate these quantities to the rms variation of the refractive index as follows. For slight index differences we have

$$n^2 - n_0^2 = 2n_1(n - n_0). \tag{39}$$

Thus we obtain from (17), using $g(r) = 1$ according to (28),

$$\langle (n - n_0)^2 \rangle = \tfrac{1}{2} (\Delta n)^2 \langle f^2(z) \rangle. \tag{40}$$

The average $\langle\ \rangle$ includes in this case also averaging over $\cos^2 \phi$. The variance $\langle f^2 \rangle$ is related to the power spectrum by the equation

$$\langle f^2 \rangle = \frac{1}{\pi} \int_0^\infty \langle |F(\theta)^2| \rangle d\theta = \frac{\theta_{\max}}{\pi} \langle |\bar{F}|^2 \rangle. \tag{41}$$

On the right-hand side of this equation we introduced the average value of the amplitudes of the spatial power spectrum $\langle |\bar{F}^2| \rangle$ and the spatial cutoff frequency $\theta_{\max}$. If we interpret $\langle |F^2| \rangle$ in (37) as the average amplitude appearing in (41) we obtain from (37) through (41)

$$[\langle (n - n_0)^2 \rangle]^{\frac{1}{2}} = 2.52 \times 10^{-4} (\theta_{\max} a)^{\frac{1}{2}}. \tag{42}$$

With $\theta_{\max} a = 0.15$ of Fig. 2 we obtain finally

$$[\langle (n - n_0)^2 \rangle]^{\frac{1}{2}} = 10^{-4}. \tag{43}$$

For our specific example, an rms deviation of this magnitude is required to achieve a relative pulse width improvement of $R = 0.1$ (a ten-times-shorter pulse of coupled modes compared to operating without mode coupling). The spatial Fourier spectrum is assumed to be flat from zero spatial frequencies to a cutoff spatial frequency of

$$\theta_{\max} = \frac{0.15}{a} = 50 \text{ cm}^{-1}. \tag{44}$$

The shortest period appearing in the Fourier spectrum is thus

$$\Lambda = \frac{2\pi}{\theta_{\max}} = 0.13 \text{ cm}. \tag{45}$$

The index fluctuation of the narrow ring defined by (23) is of the same order of magnitude as (43) if the relation (38) holds. However, one narrow ring causes gaps in the coupling process for those modes whose nulls coincide with the position of the ring. It is thus advisable to use at least two rings.

V. SUGGESTIONS FOR THE DESIGN OF INDEX FLUCTUATIONS

The spatial Fourier spectrum with a sharp cutoff frequency shown in Fig. 1 can be generated by passing noise through a low-pass filter. Another method of producing the desired index fluctuations consists in superimposing a number of sinusoidal variations. From (17), (28), and (39) we have

$$n - n_0 = \Delta n f(z) \cos \phi. \tag{46}$$

If $f(z)$ is a superposition of sine waves with random phase we have

$$n - n_0 = \Delta n \left[\sum_{\nu=1}^{M} \sin (\Omega_\nu z + \psi_\nu) \right] \cos \phi. \tag{47}$$

The ψ_ν are random phase functions of the individual sine-wave components. As a practical matter, it is probably easiest to generate these random phases by letting the phase stay constant over a distance D at which point it makes a random jump to another constant value. We assume for the purpose of our analysis that the phases are uncorrelated among each other.

It can be shown that the power spectrum of the function $\sin (\Omega_\nu z + \psi_\nu)$ may be approximated by (see appendix)

$$\langle |F_\nu(\theta)|^2 \rangle = \frac{\sin^2 (\theta - \Omega_\nu) \frac{D}{2}}{(\theta - \Omega_\nu)^2 D}. \tag{48}$$

The total power spectrum of the function $f(z)$ is thus

$$\langle |F(\theta)|^2 \rangle = \sum_{\nu=1}^{M} \frac{\sin^2 (\theta - \Omega_\nu) \frac{D}{2}}{(\theta - \Omega_\nu)^2 D}. \tag{49}$$

D is the correlation length of the phase functions. In the case that the phases stay constant and jump randomly to a new value after a distance D, this distance is identical to the correlation length. The full width of the spectrum (48) is given by

$$\Delta\theta = \frac{4\pi}{D}. \tag{50}$$

$\Delta\theta$ is the distance between the first two zeros of the $(\sin x)/x$ function on either side of its main maximum. Since we need to fill a spectral region of width θ_{max} we need a total number of

$$M = \frac{\theta_{max} D}{4\pi} \tag{51}$$

sinusoidal components. If we use $D/a = 1{,}000$ we need with $\theta_{max} a = 0.15$, $M = 12$ sinusoidal components in (47).

The necessary amplitudes Δn of the sinusoidal index variations are obtained from (37). Since the spectral components in (49) overlap only slightly, we may use

$$\langle |F|^2 \rangle = \frac{D}{4} \tag{52}$$

at the peak of each sinusoidal contribution. Using the numerical value of (37) we thus have

$$\Delta n = 1.3 \times 10^{-3} \left(\frac{a}{D} \right)^{\frac{1}{2}}. \tag{53}$$

With $D/a = 1{,}000$ we would thus have $\Delta n = 4 \times 10^{-5}$.

It is clear from our treatment that the numbers given here are only valid to an order of magnitude because of the many approximations that were made for their derivation.

The implementation of this prescription for the desired index fluctuations to the design of a fiber is not a trivial matter.

If the refractive-index increase of the core material is achieved by a doping process, it may be possible to program the doping procedure to result in the desired fluctuations. Some processes add the dopant in the gaseous phase to the material of the fiber preform. In this case it may be possible to control the flow of dopant at a predetermined rate that

is synthesized as the superposition of sine waves shown in (47). If the fiber preform is treated in this way, it would be necessary to compress the periods of the sine waves in such a way that the desired periods result after the drawing process. As mentioned earlier, the desired Fourier spectrum can also be derived from filtered electrical noise signals.

VI. DISCUSSION

We have studied the possibility of reducing multimode pulse dispersion by means of introducing refractive-index fluctuations into the core of the fiber. Several requirements must be imposed. The coupling process must be able to couple all modes of as large a mode group as possible among each other without coupling to the modes of the continuous spectrum. To achieve this, it is necessary to limit coupling to the modes inside of the area of guided modes in the mode-number plane. Modes near the outer edge of this range should remain uncoupled to avoid radiation losses. This goal can be achieved only by designing the coupling mechanism so that a definite selection rule is imposed. For simplicity we considered index fluctuation with an azimuthal dependence of the form $\cos \phi$. This azimuthal index distribution ensures that a mode with azimuthal mode number ν couples only to modes with $\nu + 1$ and $\nu - 1$. Once this selection rule is imposed, it is possible to limit coupling to modes inside of an area in mode-number space not including its outer edge. The boundary delineating the area of coupled modes in the mode-number plane tends to cross the boundary enclosing all guided modes at large values of ν. Thus the danger exists that power outflow to radiation modes occurs via modes with large ν values. This remaining problem can be avoided by limiting the intentional index fluctuations to a region inside the fiber core that remains below a certain radius $r < r_{max} < a$.

The spectrum of spatial frequencies of the z-dependent part of the coupling process must extend from (essentially) zero to a cutoff value θ_{max}. A prescription for finding θ_{max} was given in the section on the spatial Fourier spectrum. In principle, this spectrum can be synthesized as a superposition of sinusoidal components with random phase. This problem is discussed in the section on design suggestions for index fluctuations.

Our procedure leaves one question unanswered: What happens to those modes that remain intentionally uncoupled, don't they broaden the impulse response of the fiber? These modes may be naturally more heavily attenuated than the coupled modes because of their proximity

to the cutoff region in mode-number space. However, if the naturally occurring losses are insufficient to suppress these modes, steps must be taken to filter them out. This filtering is possible either by constricting the fiber at the receiver or by using spatial filtering of the radiation escaping from the end of the fiber prior to entering the detector. A reduction of the fiber diameter reduces the V value of eq. (3). Figure 2 shows a solid line labeled ($V = 30$). In the constricted fiber this line becomes the new mode boundary. It is clear that the constriction removes all the uncoupled modes in addition to some of the coupled ones. An additional amount of loss must be tolerated as payment for the pulse cleaning operation. The total number of guided modes supported by the fiber is given as[1,3]

$$N_t = \frac{V^2}{2}. \tag{54}$$

As the V value is reduced from 40 to 30 the mode number drops from 800 to 450. We lose roughly half the power in the attempt to clean up the pulse distortion that results from the free-running, uncoupled pulses. However, this 3-dB loss penalty is independent of fiber length and may be well worth paying in return for a considerable reduction of pulse dispersion. The conditions of Fig. 3 are far less favorable, here about 75 percent of the power would be lost.

Practical implementation of these ideas will tax the ingenuity of the fiber designer. Introducing desired index fluctuations with the required sharp cutoff of their spatial Fourier spectrum is an exacting requirement. The cutoff frequency θ_{max} must be kept to within a few percent. This means that the spectrum must terminate with a sharp slope. If the spectrum is synthesized as a superposition of sine waves we must require that

$$\frac{\Delta\theta}{\theta_{max}} = \frac{4\pi}{D\theta_{max}} = \frac{1}{M} < 0.01. \tag{55}$$

The number 0.01 was chosen arbitrarily, but it is certainly of the correct order of magnitude, $\Delta\theta$ was obtained from (50) and M from (51). This estimate shows that approximately 100 sinusoidal components are required to ensure that the spectrum has a sufficiently steep slope at its cutoff point. Of course, this requirement could be somewhat relaxed by allowing the sinusoidal components deeper inside the spectrum to be broader than those near its edge. These considerations may enter into the compromise that the designer wishes to achieve.

The mode spacing (in β space) changes as the fiber is bent. The modes of a dielectric slab waveguide have smaller mode spacing in

circularly bent sections of the guide. In principle, this effect could alter our conclusions regarding the possibility of uncoupling high-order modes near cutoff by limiting the width of the spatial Fourier spectrum of the coupling function. However, for the numerical example used in our discussions, the change in mode spacing due to waveguide curvature is unimportant for bent slabs whose radii remain about the limit

$$R_c > 1{,}000a.$$

For $a = 30\ \mu$m, R_c would have to be kept larger than 3 cm. It is not known if the numbers for the round fiber would be identical to the slab model, but one may expect that waveguide curvature is unimportant if the radius of curvature remains larger than a few centimeters.

APPENDIX

We provide a simple derivation of eq. (28). Let

$$f(z) = \sin [\Omega z + \psi(z)]. \tag{56}$$

The phase function $\psi(z)$ is assumed to be constant over a distance D but jumps randomly to a new constant value at the end of each interval. The Fourier transform of $f(z)$ is

$$\begin{aligned} F(\theta) &= \frac{1}{\sqrt{L}} \sum_{n=0}^{m-1} \int_{nD}^{(n+1)D} \sin [\Omega z + \psi_n] e^{-i\theta z} dz \\ &= \frac{1}{\sqrt{L}} \sum_{n=0}^{m-1} e^{i\psi_n} e^{i(\Omega-\theta)(n+\frac{1}{2})D} \frac{\sin\left[(\Omega - \theta)\frac{D}{2}\right]}{i(\Omega - \theta)}. \end{aligned} \tag{57}$$

A term with $\Omega + \theta$ has been neglected since its contribution for large values of D is negligible. It is also assumed that L is an integral multiple of D,

$$L = mD. \tag{58}$$

When we form the absolute-square value of F and take the ensemble average, all cross terms in the resulting double summation vanish because of our assumption of random values for ψ_n. The phase terms in the remaining terms of the summation reduce to unity by the process of taking the absolute-square value. With no summation index left under the summation sign, the sum results simply in a factor m. Using (58) we finally obtain

$$\langle |F(\theta)|^2 \rangle = \frac{\sin^2\left[(\theta - \Omega)\frac{D}{2}\right]}{(\theta - \Omega)^2 D}. \tag{59}$$

REFERENCES

1. D. Gloge, "Weakly Guiding Fibers," Appl. Opt., *10*, No. 10 (October 1971), pp. 2252–2258.
2. D. Gloge, "Dispersion in Weakly Guiding Fibers," Appl. Opt., *10*, No. 11 (November 1971), pp. 2442–2445.
3. D. Marcuse, *Theory of Dielectric Optical Waveguides*, New York: Academic Press, 1974.
4. S. D. Personick, "Time Dispersion in Dielectric Waveguides," B.S.T.J., *50*, No. 3 (March 1971), pp. 843–859.
5. D. Marcuse, "Pulse Propagation in Multimode Dielectric Waveguides," B.S.T.J., *51*, No. 6 (July-August 1972), pp. 1199–1232.
6. D. Marcuse, *Light Transmission Optics*, New York: Van Nostrand-Reinhold Co., 1972.
7. M. Abromovitz and I. A. Stegun, *Handbook of Mathematical Functions with Formulas, Graphs and Mathematical Tables*, National Bureau of Standards Applied Mathematics Series, *55*, National Bureau of Standards, Washington, D. C., 1965.
8. Ref. 3, eq. (4.7-5), p. 168.
9. Ref. 3, Section 3.6.
10. Ref. 3, eq. (5.5-25), p. 206.
11. Ref. 3, eq. (5.5-45) and (5.5-55), pp. 209–210.
12. D. Gloge, "Optical Power Flow in Multimode Fibers," B.S.T.J., *51*, No. 8 (October 1972), pp. 1767–1783.